



## A catalogue of up to 26 known exoplanets accessible to reflected-starlight observations with the Roman Space Telescope

Óscar Carrión-González<sup>1</sup>, Antonio García Muñoz<sup>1,2</sup>, Nuno C. Santos<sup>3,4</sup>, Juan Cabrera<sup>5</sup>, Szilárd Csizmadia<sup>5</sup>, and Heike Rauer<sup>1,5,6</sup>

<sup>1</sup>Technische Universität Berlin, Physikalische Institute, Zentrum für Astronomie und Astrophysik, Berlin, Germany (o.carriongonzalez@astro.physik.tu-berlin.de)

<sup>2</sup>AIM, CEA, CNRS, Université Paris-Saclay, Université de Paris, Gif-sur-Yvette, France

<sup>3</sup>Instituto de Astrofísica e Ciências do Espaço, Universidade do Porto, CAUP, Porto, Portugal

<sup>4</sup>Departamento de Física e Astronomia, Faculdade de Ciências, Universidade do Porto, Porto, Portugal

<sup>5</sup>Deutsches Zentrum für Luft- und Raumfahrt, Berlin, Germany

<sup>6</sup>Institute of Geological Sciences, Freie Universität Berlin, Berlin, Germany

### Abstract

The coronagraph instrument aboard the Nancy Grace Roman Space Telescope is a technology demonstrator that will perform the first reflected-starlight direct imaging observations of exoplanets. This instrument will pave the way for future missions such as LUVOIR or HabEx, which have the goal of characterizing the atmospheres of Earth-like exoplanets. In this work we develop a statistical method to compute which of the confirmed exoplanets in the NASA Exoplanet Archive would be accessible in reflected starlight to a direct-imaging telescope. By applying our method to the Roman Telescope's coronagraph, we show that an eventual science phase of the Roman Telescope's coronagraph has a remarkable potential to study cold and temperate exoplanets and initiate their atmospheric characterization.

### Introduction

The years until the expected launch of the Roman Telescope<sup>[1]</sup> in 2025 should be used to improve the orbital characterization of the most interesting targets through radial velocity or astrometry campaigns. For this, a target list of known exoplanets that could be observed with the Roman Telescope's coronagraph is needed. Additional figures describing the detectability and scientific interest of each accessible exoplanet are useful to prioritize the observations of the targets.

### Statistical method

We use the NASA Exoplanet Archive<sup>[2]</sup> as the main source of information for the planetary and stellar properties of each of the about 4300 confirmed exoplanets. For each exoplanet, we compute 10,000 orbital realizations letting each of the parameters involved vary within its reported upper and lower uncertainties. When the orbital inclination ( $i$ ), the eccentricity ( $e$ ) or the argument of

periastron of the planet ( $\omega_p$ ) are unconstrained, we randomly draw their value at each orbital realization from uniform distributions. When the planet radius is unknown, we compute it by means of published mass-radius relationships<sup>[3][4]</sup>. By discretizing each orbital realization into 360 positions, we compute at each position the angular separation between the planet and the star ( $\Delta\theta$ ) and the planet-to-star contrast ratio ( $F_p/F_*$ ). We define a planet as Roman-accessible if at a certain orbital position its angular separation is within the inner and the outer working angles (IWA, OWA) of the coronagraph and, additionally, the planet-to-star contrast is brighter than the minimum contrast ( $C_{\min}$ ) that the coronagraph can detect.

Our main outputs are the probability of a planet to be Roman-accessible ( $P_{\text{access}}$ ), the range of observable phase angles ( $\alpha_{\text{obs}}$ ), the number of days per orbit in which the planet is accessible ( $t_{\text{obs}}$ ) and its transit probability. Due to its interest for atmospheric modelling, we also compute the equilibrium temperature ( $T_{\text{eq}}$ ) at each orbital position. This allows us to compute the mean value of  $T_{\text{eq}}$  throughout the orbit, its variation due to orbital eccentricity and the variation of  $T_{\text{eq}}$  that takes place while the planet is accessible, which could result in detectable atmospheric variability.

With this method, we computed the accessibility of each planet at wavelengths 575, 730 and 825 nm, consistent with the coronagraph filters that are currently commissioned. We repeated this study for three plausible configurations of the coronagraph because its final design is not yet completed. We label these configurations as optimistic (IWA=3 $\lambda$ /D, OWA=9 $\lambda$ /D,  $C_{\min}=1\times 10^{-9}$ ), intermediate (IWA=3.5 $\lambda$ /D, OWA=8.5 $\lambda$ /D,  $C_{\min}=3\times 10^{-9}$ ) and pessimistic (IWA=4 $\lambda$ /D, OWA=8 $\lambda$ /D,  $C_{\min}=5\times 10^{-9}$ ).

## Results

We find up to 26 exoplanets Roman-accessible exoplanets in the optimistic scenario with  $P_{\text{access}}>25\%$  and orbiting stars brighter than  $V=7$  mag<sup>[5]</sup>. We apply the latter two vetting criteria throughout our work due to the particular constraints of the Roman Telescope mission timeline and the sensitivity of its coronagraph instrument. This number of Roman-accessible exoplanets is reduced to 10 and 3 in the intermediate and pessimistic scenarios, respectively.

For the Roman-accessible exoplanets in the optimistic scenario we carried out a population study and found that this set of planets is dominated by giant exoplanets more massive than Jupiter. Interestingly, it also includes the low-mass planets tau Cet e and f, which orbit near the habitable zone of their host star. These two planets are however barely accessible in the intermediate or pessimistic coronagraph scenarios (Fig. 1). Thirteen of the 26 Roman-accessible exoplanets are part of multi-planet systems and three of them have inner companions observed in transit, which would enable the simultaneous characterization of the inner and the outer regions of these planetary systems. The mean equilibrium temperatures of the Roman-accessible planets range from values in the order of that of Uranus to values above 400 K, including some targets at  $\sim 300$  K (Fig. 2).

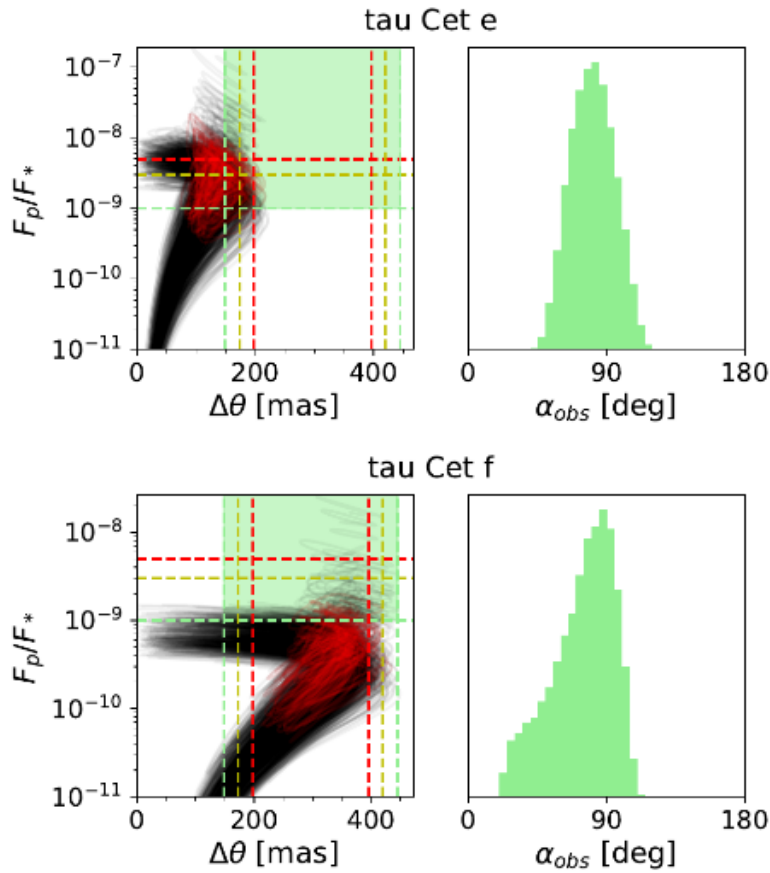


**Fig. 1.** Detectability of tau Cet e and f in the optimistic CGI configuration (green dashed lines), the intermediate (yellow dashed lines) and pessimistic one (red dashed lines). In the left panels, black lines correspond to orbital realizations without an inclination constraint. Solid red lines correspond to orbital configurations with  $25^\circ < i < 45^\circ$ , coplanar with the debris disc of the system (Lawler et al. 2014). For this case, the inclination is sampled from a uniform distribution within the quoted limits. The green histograms in the right panels show the posterior distributions of  $\alpha_{obs}$  in the optimistic CGI configuration.

For a selection of particularly interesting targets, we analysed in more detail the prospects for observing and eventually characterizing these planets. For instance, we discussed how the detectability prospects may change if additional constraints on the orbital inclination are set e.g. with astrometry (Fig. 1).

We find some exoplanets with remarkably wide ranges of observable phase angles, which makes them interesting for atmospheric characterization with reflected-starlight phase curves<sup>[6]</sup>. In this regard, we also discussed the importance of consistently reporting the planet and stellar parameters in exoplanet catalogues such as the NASA Archive and the misleading detectability results that might be achieved if an A standardization process is not performed.

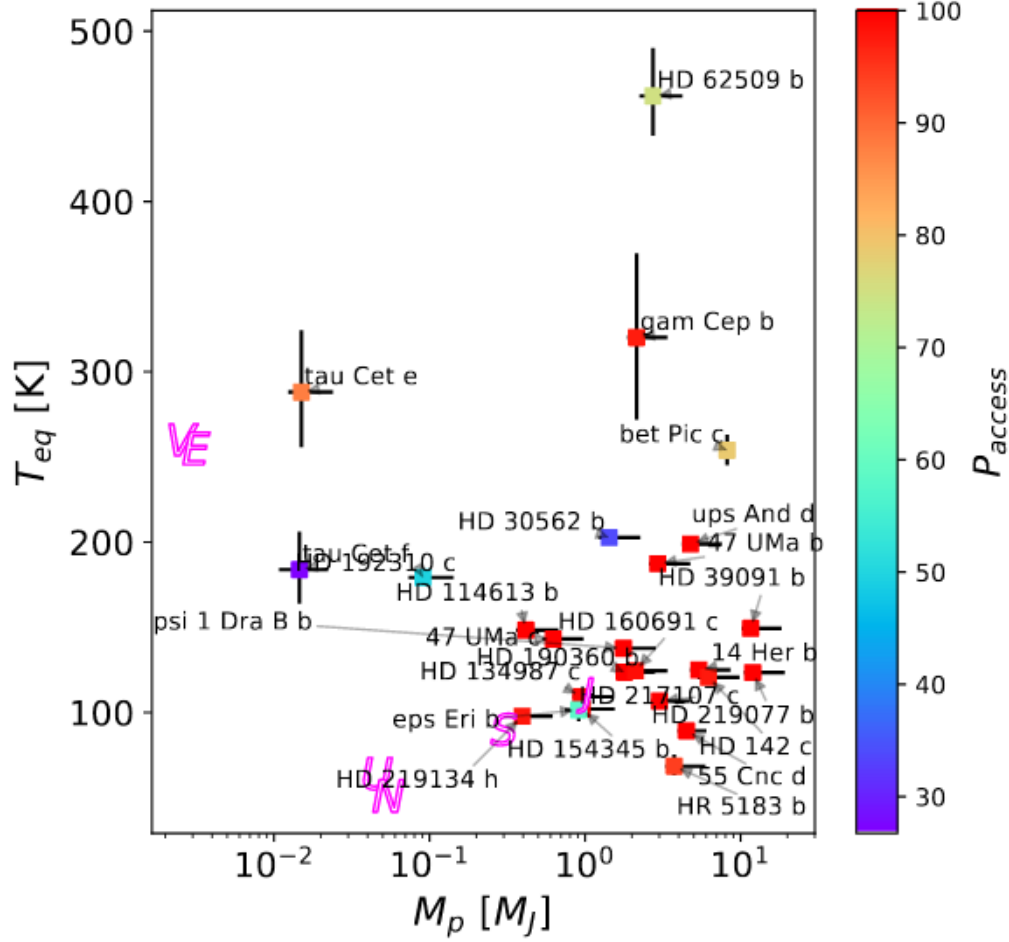


**Fig. 2.** Median  $T_{eq}$  against the median  $M_p$  for each Roman-accessible planet in the optimistic CGI configuration as computed in our 10000 orbital realizations. The colour of the markers indicates the  $P_{access}$  of the exoplanet. Horizontal and vertical error bars correspond to the upper and lower uncertainties of  $M_p$  and  $T_{eq}$ , respectively. Magenta letters in the diagram indicate the Solar System planets Venus (V), Earth (E), Jupiter (J), Saturn (S), Uranus (U), and Neptune (N).

Overall, we find that a science phase of the Roman Telescope’s coronagraph would have an extraordinary potential to perform one-of-a-kind observations before next-generation missions that are not expected at least until the mid-2030s.

## References

- [1] Spergel et al. (2013), <https://arxiv.org/abs/1305.5422>
- [2] Akeson et al. (2013), *PASP*, 125, 989
- [3] Hatzes & Rauer (2015), *ApJL*, 810, L25
- [4] Otegi et al. (2020), *A&A*, 634, A43
- [5] Carrión-González et al. (2021), *A&A* accepted
- [6] Carrión-González et al. (2021), in prep.

